Transactions, SMiRT-22
San Francisco, California, USA - August 18-23, 2013
Division V

MECHANICAL PROPERTIES OF ELASTOMERIC SEISMIC ISOLATION BEARINGS FOR ANALYSIS UNDER EXTREME LOADINGS

Manish Kumar[1], Andrew S. Whittaker[2,3] and Michael C. Constantinou[2]

[1] Graduate student, Department of Civil Engineering, University at Buffalo, NY (mkumar2@buffalo.edu)
[2] Professor, Department of Civil Engineering, University at Buffalo, NY
[3] Director, Multidisciplinary Center for Earthquake Engineering Research (MCEER)

ABSTRACT

The nuclear accident at Fukushima Daiichi in March 2011 has led the nuclear community to consider the effects of beyond design basis loadings, including extreme earthquakes. Seismic isolation is being considered for new large light water and small modular reactors, and isolation-system designs will have to consider these extreme loadings. The United States Nuclear Regulatory Commission (USNRC) is sponsoring a research project that will quantify the response of low damping rubber (LDR) and lead-rubber (LR) bearings under loadings associated with extreme earthquakes. Under design basis loadings, the response of an elastomeric bearing is not expected to deviate from well-established numerical models and bearings are not expected to experience net tension. However, under extended or beyond design basis shaking, elastomer shear strains may exceed 300% in regions of high seismic hazard, bearings may experience net tension, the compression and tension stiffness will be affected by isolator lateral displacement, and the properties of the lead core in LR bearings will degrade due to substantial energy dissipation.

Phenomenological models are presented to describe the behavior of elastomeric isolation bearings in compression and tension, explicitly considering both the effects of lateral displacement and cyclic vertical and horizontal loading. The numerical models are coded in OpenSees and described in the paper. Results of numerical analysis are compared with test data to validate the numerical models.

INTRODUCTION

The behavior of elastomeric bearings in shear and compression is well established, and mathematical models exist to reasonably capture the response expected for design basis earthquake. These mathematical models use simplified load-deformation relationships and ignore behaviors that might be important under beyond design basis earthquakes during which elastomeric bearings experience large strains under three-dimensional loading. These properties are discussed here and existing mathematical models are extended to include the effects of these properties on the response of elastomeric bearings.

Knowledge of the tensile properties of elastomeric bearing is rather limited and the available mathematical models do not capture the experimentally observed behavior in tension. Constantinou et al. (2007) recommended the two-spring model of Koh and Kelly (1987) for vertical stiffness in compression, which has been validated experimentally by Warn et al. (2007), and a bilinear model in tension having the same stiffness as in compression up to the point of cavitation. Yamamoto et al. (2009) used a similar backbone curve as in Constantinou et al. (2007) and included hysteresis in compression and tension. This model uses the compression modulus proposed by Gent and Lindley (1959) and an arbitrarily small value of post-cavitation modulus. This model ignores permanent damage, reduction in cavitation strength, and effect of loading history, which might be of importance for beyond design basis earthquake loadings. In addition to the models discussed above, other researchers have proposed empirical formulae for stiffness and cavitation strength (e.g., Iwabe *et al.*, 2000; Yang *et al.*, 2010). However, these formulae are based on

limited experimental results and a robust mathematical formulation for use in structural analysis cannot be obtained from these models.

The tensile properties of seismic isolation elastomeric bearings are discussed in this paper and new phenomenological models are proposed that capture the response of these bearings.

MECHANICAL BEHAVIOR IN VERTICAL DIRECTION

Coupling of Horizontal and Vertical Motion

The dependence of axial stiffness on lateral displacement is captured by the two-spring (Koh and Kelly, 1987). The two-spring model has been validated experimentally by Warn *et al.* (2007) and used here owing to its robust formulation and ease of numerical implementation. The vertical stiffness of the elastomeric bearing obtained from the two-spring model is given as:

$$K_v = \frac{AE_c}{T_r}\left[1+\frac{3}{\pi^2}\left(\frac{u}{r}\right)^2\right]^{-1} \tag{1}$$

where A is the bonded rubber area, E_c is the compression modulus of the bearing, T_r is the total rubber thickness, u is the lateral displacement of the bearing, and r is the radius of gyration of the bonded rubber area. The effect of coupling of vertical stiffness and lateral displacement on axial load-deformation curve is softening near the critical buckling load, shown with the dotted lines in Figure 1.

Buckling in Compression

The critical buckling, P_{cr}, load in compression is given by the expression derived in the two-spring model (Koh and Kelly, 1987). P_{cr} decreases with increasing lateral displacement. The area-reduction method considers the dependence of P_{cr} on lateral displacement and provides conservative results (e.g., Buckle *et al.*, 2002; Warn *et al.*, 2007). The reduced critical buckling load is given by $P'_{cr} = P_{cr}(A_r / A)$, where A_r is the reduced area of a bearing of diameter B due to lateral displacement D. The area-reduction method suggests zero capacity for a bearing at a horizontal displacement equal to the diameter (or width) of bearing. However, experiments have shown that a bearing does not lose all its capacity but maintains a minimum capacity after the overlapping area reduces to zero (Warn *et al.*, 2007). The model proposed by Warn *et al.* (2007) is considered here, which uses a bilinear approximation of the area-reduction method and takes into account the finite buckling capacity of a bearing at zero overlap area. The piecewise linear approximation of the area-reduction model is illustrated in Figure 2.

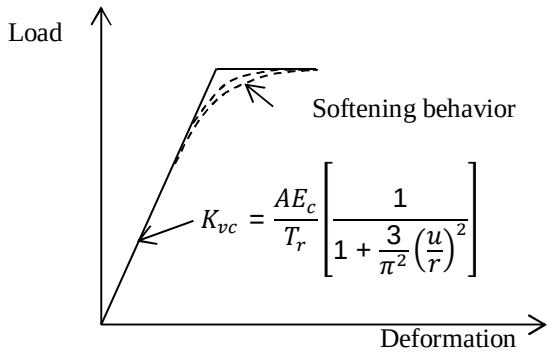

Figure 1. Stress softening under compression

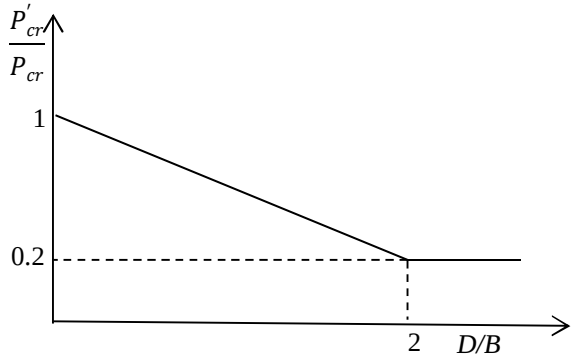

Figure 2. Piecewise linear model in compression

Cavitation in Tension

Cavitation is followed by the substantial reduction in the vertical stiffness indicated by highly discernible transition on the tensile load-deformation curve. Gent (1990) suggested that cavitation occurs at a negative pressure of about $3G$, and the cavitation force F_c is given by the expression $3GA_o$, where A_o is the bonded rubber area and G is the shear modulus of rubber obtained experimentally from the testing of elastomeric bearings at large shear deformations under nominal axial loads.

Post-cavitation Behavior

Most of the available mathematical models use a very small arbitrary value of post-cavitation stiffness. Constantinou et al. (2007) suggested the following expression for post-cavitation stiffness:

$$K_{post-cavitation} = \frac{EA}{T_r} \tag{2}$$

where E is the elastic modulus of rubber. Following the formation of cracks in the rubber layer of elastomeric bearing after cavitation, rubber loses its triaxial state of stress and experiences uniaxial tensile stress. Hence, the elastic modulus used in Equation (2) is the Young's modulus of rubber.

Experiments have shown that the post-cavitation stiffness of elastomeric bearings decreases with increasing tensile deformation. It is assumed here that area used in Equation (2) is the "true area" of bearing excluding the total area of cavities that change with tensile deformation. If the rubber area is considered to be made up of infinite number of small area elements, every time a cavity is formed, an area element is eroded. The greater the area, the greater the rate of destruction of area elements. So the rate of reduction of true area with respect to tensile deformation would be proportional to the instantaneous true area at any moment, which can be expressed mathematically as:

$$\frac{\partial A}{\partial u} = -kA \tag{3}$$

where k is defined as cavitation parameter, which is constant for a particular elastomeric bearing and describes the post-cavitation variation of tensile stiffness and area. Equations (2) and (3) produce set of differential equations for post-cavitation behavior. These sets of differential equations are solved using initial conditions at the onset of cavitation $\left(F_c, u_c, \sigma_c, \varepsilon_c, A_o\right)$ to obtain the current state $\left(F, u, \sigma, \varepsilon, A\right)$ as:

$$A = A_o e^{-k(u-u_c)} \tag{4}$$

$$F = F_c\left[1 + \frac{1}{kT_r}\left(1 - e^{-k(u-u_c)}\right)\right] \tag{5}$$

$$\sigma = \sigma_c\left[e^{kT_r(\varepsilon-\varepsilon_c)} + \frac{1}{kT_r}\left(e^{kT_r(\varepsilon-\varepsilon_c)} - 1\right)\right] \tag{6}$$

where $\sigma_c = 3G$ is the cavitation stress and $F_c = 3GA_o$ is the cavitation strength of the bearing. The variation of tensile force with tensile deformation is shown in Figure 3. The constant k is obtained using experimental data.

Strength Degradation in Cyclic Loading

Cavitation in elastomeric bearings is accompanied by the irreversible damage due to formation of micro cracks in the volume of rubber. When bearing is loaded beyond the point of cavitation and unloaded, it returns along a new path and cavitation strength is reduced. The area enclosed between loading and unloading amounts to the hysteretic energy due to damage in the bearing. Subsequent loading follows the latest unloading path elastically until strain exceeds the past maximum value $u_{\max}$, below which loading has the effect of only opening and closing of existing cavities within the rubber. Once loading exceeds the past maximum value of tensile strain, the formation of new cavities leads to increased damage, and follows the post cavitation behavior defined previously by Equation (5). Upon load reversal, it again traces back a new unloading path and cavitation strength is reduced. Unloading paths can be approximated with a straight lines between the point of maximum strain $(F_{\max}, u_{\max})$ to the point of reduced cavitation strength (F_{cn}, u_{cn}). These points change with increasing number of cycles. To capture this behavior mathematically, a damage index ϕ is defined such that the updated cavitation strength as a function of initial cavitation strength is given by the expression:

$$F_{cn} = F_c(1-\phi) \tag{7}$$

The damage index ϕ represents the cumulative damage in the bearing $(0 \le \phi \le 1)$. It is a function of maximum deformation experienced by the bearing under tensile loading. Mathematically it can be expressed as $\phi = f(u_{\max})$, where f satisfies the following relations: 1) $f(u_c) = 0$ (No strength reduction up to cavitation deformation), and 2) $f(u_{\max}) \to \phi_{\max}$ (Damage index converges to a maximum value after large deformations). A function satisfying these properties is given by:

$$\phi = \phi_{\max}\left[1 - e^{-a\left(\frac{u-u_c}{u_c}\right)}\right] \tag{8}$$

where a is the strength degradation parameter that defines the rate of damage and $\phi_{\max}$ is the maximum damage that can be expected in a bearing. The load-deformation behavior of elastomeric bearings under cyclic tensile loading is summarized in Figure 4.

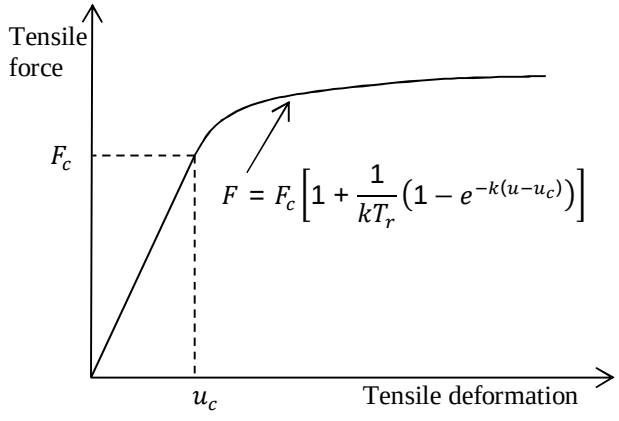

Figure 3. Post-cavitation behavior

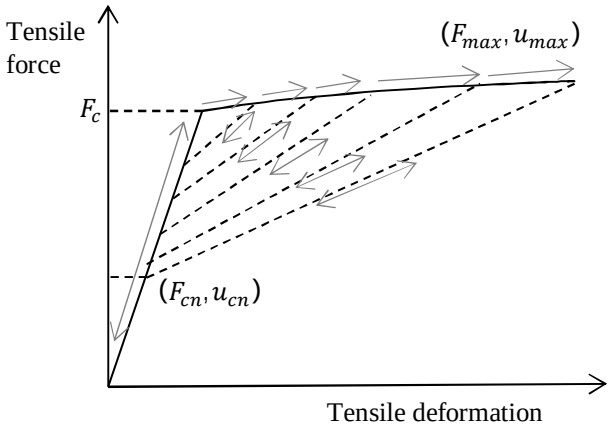

Figure 4. Strength reduction under cyclic loading

Mathematical Model in Axial Direction

A mathematical model of an elastomeric bearing in the axial direction is presented in Figure 5, which captures the following characteristics in the axial direction: 1) buckling in compression, 2) coupling of vertical and horizontal motion, 3) cavitation, 4) post-cavitation variation, and 5) strength degradation due to cyclic loading. The model uses three unknown parameters: 1) a cavitation parameter, k, 2) a strength degradation parameter, a, and 3) a damage index, $\phi_{\max}$.

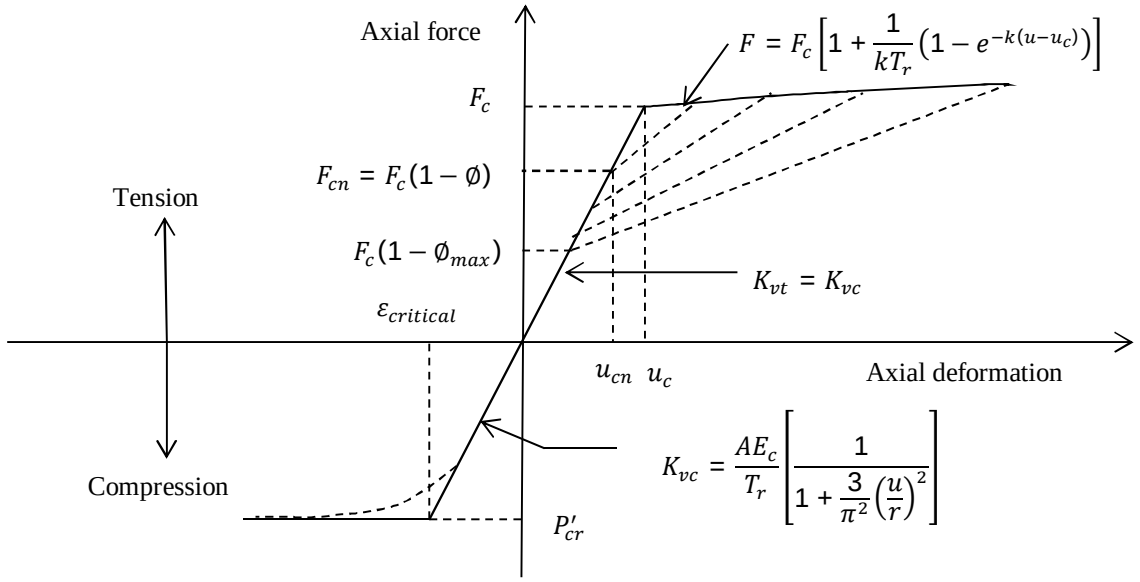

Figure 5. Mathematical model of elastomeric bearings in axial direction

MECHNANICAL BEHAVIOR IN SHEAR

Coupled Horizontal Response

A smooth hysteretic model is used for elastomeric bearings in horizontal shear, which is shown in Figure 6. It is based on the model proposed by Park et al. (1986) and extended for the analysis of elastomeric bearings under bidirectional motion.

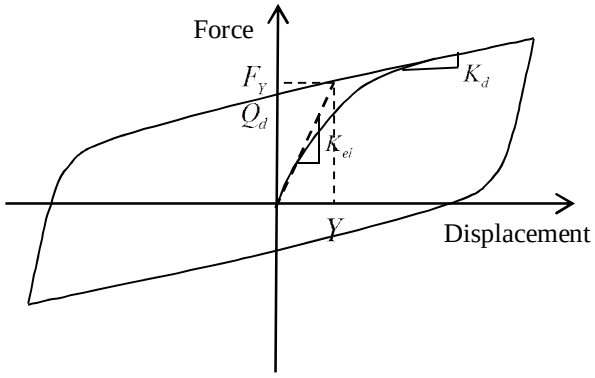

Figure 6. Mathematical model in shear

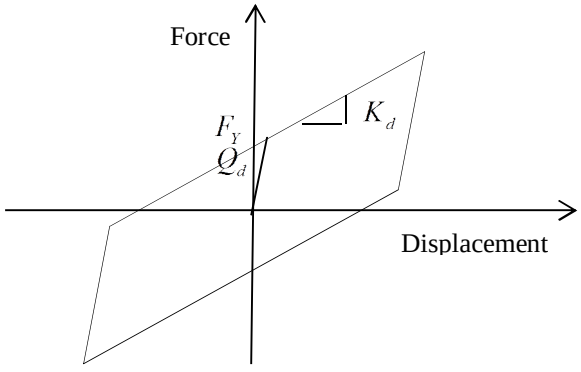

Figure 7. Idealized behavior in shear

Parameters have been expressed here in the form that is typical of seismic isolation design, namely, initial elastic stiffness K_{el}, characteristic strength Q_d, yield strength F_Y, yield displacement Y, and post-elastic stiffness K_d. The isotropic formulation of the model in terms of restoring forces in orthogonal directions, F_x and F_y, is given by the equation (Mokha *et al.*, 1993; Nagarajaiah *et al.*, 1989):

$$\begin{Bmatrix} F_x \\ F_y \end{Bmatrix} = c_d \begin{Bmatrix} \dot{U}_x \\ \dot{U}_y \end{Bmatrix} + K_d \begin{Bmatrix} U_x \\ U_y \end{Bmatrix} + \left(\sigma_{YL} A_L\right) \begin{Bmatrix} Z_x \\ Z_y \end{Bmatrix} \tag{9}$$

where σ_{YL} is the effective yield stress of confined rubber, A_L is the cross-sectional area of lead-core, and c_d is a parameter that accounts for the viscous energy dissipation in rubber. Z_x and Z_y represents the hysteretic component of the restoring forces. Both have units of displacement and are function of time histories of u_x and u_y. The biaxial interaction is given by the following differential equation:

$$Y \begin{Bmatrix} \dot{Z}_x \\ \dot{Z}_y \end{Bmatrix} = \left(A[I] - \begin{bmatrix} Z_x^2 \left(\gamma Sign\left(\dot{U}_x Z_x\right) + \beta\right) & Z_x Z_y \left(\gamma Sign\left(\dot{U}_y Z_y\right) + \beta\right) \\ Z_x Z_y \left(\gamma Sign\left(\dot{U}_x Z_x\right) + \beta\right) & Z_y^2 \left(\gamma Sign\left(\dot{U}_y Z_y\right) + \beta\right) \end{bmatrix} \right) \begin{Bmatrix} \dot{U}_x \\ \dot{U}_y \end{Bmatrix} \tag{10}$$

Parameters γ and β control the shape of the hysteresis loop and A is the amplitude of the restoring force.

Heating of lead-core

For LR bearings, the effective yield stress of lead used in Equation (9) is not constant but decreases with the number of cycles due to heating of the lead core under large cyclic displacements. The extent of reduction depends on the geometric properties of bearing and speed of motion. Kalpakidis *et al.* (2010) proposed a dependency of the characteristic strength of LR bearings on instantaneous temperature of lead core, which itself is a function of time. The sets of equations proposed by Kalpakidis *et al.* (2010) is used here to describe heating of the lead core.

Equivalent damping

The damping in LR bearings is primarily contributed by the energy dissipation in the lead core and the contribution of viscous damping in the rubber is typically neglected. The force-displacement loop of an elastomeric bearing is idealized as in Figure 7, and the effective period and effective damping of the isolation system are calculated using following set of equations (AASHTO, 2010; ASCE, 2010):

$$T_{eff} = 2\pi \sqrt{\frac{W}{K_{eff} g}}; K_{eff} = K_d + \frac{Q_d}{D}; \beta_{eff} = \frac{1}{2\pi} \left[\frac{EDC}{K_{eff} D^2} \right] \tag{11}$$

where D is the displacement of the system due to earthquake shaking obtained from smoothed response spectra, and EDC is the energy dissipated per cycle at displacement D. For the idealized behavior shown in Figure 7, EDC is given as $EDC = 4Q_d\left(D - Y\right)$, where Y is the yield displacement of the system. The characteristic strength of a LR bearing is determined using the effective yield stress of lead core. However, for LDR bearings, the characteristic strength cannot be obtained directly. An effective damping of system is assumed, and characteristic strength is determined as follows:

$$\beta_{eff} = \frac{1}{2\pi}\left[\frac{4Q_d\left(D-Y\right)}{K_{eff}D^2}\right] \le \frac{2Q_d}{\pi K_d D} \tag{12}$$

$$Q_d \ge \frac{\pi}{2} \times \beta_{eff} \times K_d \times D \tag{13}$$

The characteristic strength of LDR bearings can be estimated if the value of displacement D due to earthquake shaking is known from the simplified analysis (e.g., Constantinou *et al.*, 2011).

Variation in shear modulus

The effective shear modulus of elastomeric bearings is obtained from experimental data. LDR and LR bearings show viscoelastic and hysteresis behavior in shear, respectively. The effective stiffness, K_{eff}, at displacement amplitude D is calculated using expression $K_{eff} = (|F^+| + |F^-|)/(|\Delta^+| + |\Delta^-|)$, where Δ^+ and Δ^- are the maximum and minimum horizontal displacements obtained from an experiment, and F^+ and F^- are the corresponding forces. The effective shear modulus is determined using the expression $G_{eff} = K_{eff}T_r / A_r$. Most of the available mathematical models use a constant shear modulus for elastomeric bearing, although shear modulus varies with strain and axial loads. Increasing the axial pressure reduces the shear modulus. However, if the shear modulus, G, is determined from testing of elastomeric bearings at large strains and under nominal axial pressure, the value of G already includes some effects of axial load. Moreover, Constantinou *et al.* (2007) report that effect of axial load on shear stiffness is negligible. A typical variation of shear modulus with strain under different nominal axial pressures is shown in Figure 8 for a LDR bearing of diameter 35.5 inch (shape factor = 26).

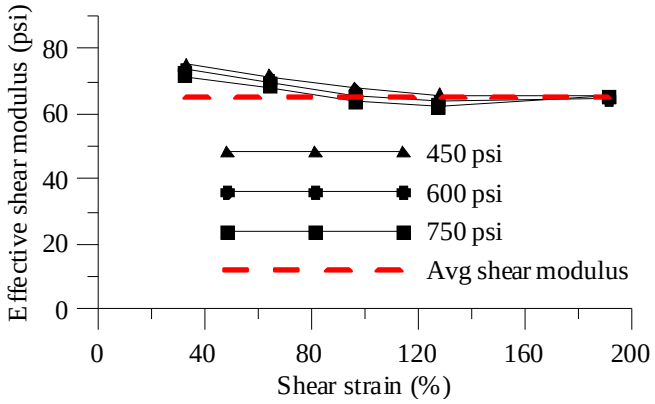

Figure 8. Stress and strain dependency of LDR bearings (courtesy of DIS Inc.)

The shear modulus of natural rubber decreases with increasing strain up to 100%, remains relatively constant for shear strain between 100 and 200%, and increases again at shear strains of 200 to 250%. The shear modulus obtained from testing of elastomeric bearings at large strains is used for horizontal stiffness (LDR bearings), post-elastic stiffness (LR bearings), and buckling load calculations.

Mathematical model in shear

The mathematical model presented in Figure 6 captures the following characteristics of lead-rubber bearings: 1) nonlinear shear force-deformation behavior, 2) bi-directional interaction in the horizontal plane, and 3) strength degradation due to heating of the lead core in LR bearings.

For numerical implementation, the model is represented as sum of two sub-models: 1) a viscoelastic model of rubber, and 2) an elasto-plastic model of lead. The contribution of the rubber to the total resisting force is given by the first two terms in Equation (9) and the third term represents the contribution of the lead core. The sum of all three terms is the restoring force in the LR bearing. For LR bearings, the characteristic strength, or the yield stress of the lead core, decreases with the number of cycles under large shear deformation. The yield stress of the lead core at the reference temperature (beginning of motion) is obtained experimentally as it depends on the degree of confinement of the lead core in the bearing. A suitable value of yield displacement of the lead core can be assumed, often between $0.05T_r$ to $0.1T_r$. It should be noted that small variations in the yield displacement do not substantially affect the displacement response of an isolated structure. For LDR bearings the hysteretic term in Equation (9) is replaced by the yield strength of the LDR bearing obtained using the assumed value of effective damping of the system.

MECHANICAL BEHAVIOR IN ROTATION AND TORSION

The torsional and rotational behaviors of individual elastomeric bearings do not significantly affect the overall response of a seismically isolated structure. Hence, behavior in rotation and torsion are represented by linear elastic springs with stiffnesses given as $K_r = E_r I_s / T_r$ and $K_t = GI_t / T_r$, respectively, where, E_r is the rotation modulus of the bearing, I_s is the moment of inertia about axis of rotation in the horizontal plane, and I_t is the moment of inertia about the vertical axis.

COMPARISON WITH THE EXPERIMENTAL DATA

The mathematical models of elastomeric bearing were implemented in the software program OpenSees (McKenna *et al.*, 2006) as two new User Elements for LDR and LR bearings. The three-dimensional continuum geometry of elastomeric bearing was modeled as a 2-Node, 12 DOF discrete element. The two nodes are connected by six springs, which represent the material models in an axial, two shear, torsional and two rotational directions. Three sets of experimental data, as shown in Figure 9, were used to investigate the capability of the proposed mathematical model to simulate the behavior of elastomeric bearings under cyclic tensile loading. The cavitation parameter, k, and the damage index, $\phi_{\max}$, were obtained by calibration of the mathematical model with the experimental data. The strength degradation parameter, a, was assumed to be unity.

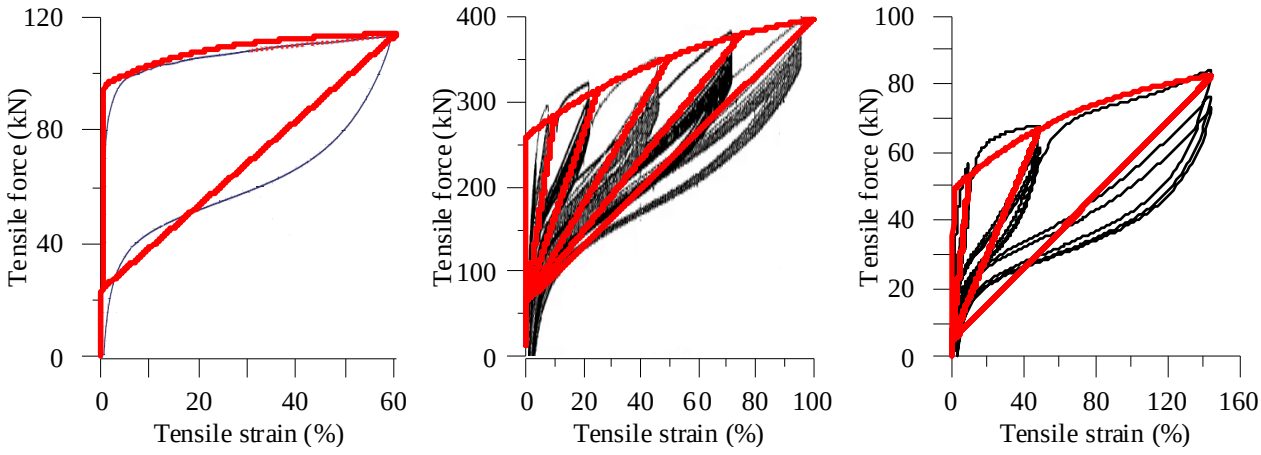

a) Constantinou et al. (2007) b) Iwabe et al. (2000) c) Warn (2006)

Figure 9. Calibration of the mathematical model with experimental response

The details of the bearings and the values of parameters estimated by calibration against experimental data are presented in Table 1.

Table 1. Properties of the bearings used for experimental comparison

	Constantinou et al. (2007)	Iwabe et al. (2000)	Warn (2006)
Diameter (mm)	250	500	164
Shape factor	9.8	33	10.2
Cavitation parameter	60	15	20
Damage index	0.75	0.75	0.9
Strength degradation parameter	1.0	1.0	1.0

The behavior of elastomeric bearings under shear and compression is well established, and the comparison of numerical results with the experimental data is not presented here. Validation of the mathematical model used for the strength degradation of LR bearings due to heating in lead core under cyclic shear loading is presented in Kalpakidis *et al.* (2010).

SUMMARY AND CONCLUSIONS

Mathematical models of LDR and LR bearings that can be used for the analysis of base isolated structures under beyond design basis shaking are presented. These mathematical models extend the available robust formulation in shear and compression, and a new phenomenological model is proposed for behavior under tension. The phenomenological model uses three unknown parameters that can be determined experimentally.

Robust numerical formulations are obtained with the mathematical models. Numerical models are implemented in OpenSees as new user elements, and numerical results compare well with the experimental data for behavior in tension. A formal model validation will require that unknown parameters of the model be obtained from experiments. In most cases, the strength degradation parameter, a, can be assumed to be unity, and the damage index, $\phi_{\max}$, will range between 0.5 and 0.9. These two parameters are not expected to have significant effect on the tensile response of an elastomeric bearing. The cavitation parameter, k, should be determined experimentally, or can be estimated based on the experimental data available for bearings of a similar shape, size, compound, and fabrication.

ACKNOWLEDGEMENTS

This research project is supported by a grant to MCEER from the United States Nuclear Regulatory Commission and the Lawrence Berkeley National Laboratory. This financial support is gratefully acknowledged. The authors thank former graduate students Dr. Yannis Kalpakidis of Energo Engineering and Dr. Gordon Warn of Penn State University for providing test data on elastomeric bearings.

REFERENCES

AASHTO (2010). "Guide specifications for seismic isolation design." American Association of State Highway and Transportation Officials, Washington, D.C.

ASCE (2010). "Minimum design loads for buildings and other structures." Reston, Va., American Society of Civil Engineers

Buckle, I., Nagarajaiah, S., and Ferrell, K. (2002). "Stability of elastomeric isolation bearings: Experimental study." *Journal of Structural Engineering*, 128(1), 3-11.

Constantinou, M., Kalpakidis, I., Filiatrault, A., and Lay, R. A. E. (2011). "LRFD-based analysis and design procedures for bridge bearings and seismic isolators." Report 11-0004, MCEER, Buffalo, NY.

Constantinou, M. C., Whittaker, A. S., Kalpakidis, Y., Fenz, D. M., and Warn, G. P. (2007). "Performance of Seismic Isolation Hardware Under Service and Seismic Loading." Report 07-0012, MCEER, Buffalo, New York, 472p.

Gent, A., and Lindley, P. (1959). "The compression of bonded rubber blocks." *Proceedings of the Institution of Mechanical Engineers* 173(1959), 111-122.

Gent, A. (1990). "Cavitation in rubber: a cautionary tale." *Rubber Chemistry and Technology*, 63, 49.

Iwabe, N., Takayama, M., Kani, N., and Wada, A. (2000). "Experimental study on the effect of tension for rubber bearings." *Proceedings: 12th World Conference on Earthquake Engineering*, New Zealand.

Kalpakidis, I. V., Constantinou, M. C., and Whittaker, A. S. (2010). "Modeling strength degradation in lead-rubber bearings under earthquake shaking." *Earthquake Engineering and Structural Dynamics*, 39(13), 1533-1549.

Koh, C. G., and Kelly, J. M. (1987). "Effects of axial load on elastomeric isolation bearings." Report No. 86/12, Earthquake Engineering Research Center, University of California, Berkeley, United States, 108p.

McKenna, F., Fenves, G., and Scott, M. (2006). Computer Program OpenSees: Open system for earthquake engineering simulation, Pacific Earthquake Engineering Center, University of California, Berkeley, CA., http://opensees.berkeley.edu.

Mokha, A. S., Constantinou, M. C., and Reinhorn, A. M. (1993). "Verification of friction model of teflon bearings under triaxial load." *Journal of structural engineering New York, N.Y.*, 119(1), 240-261.

Nagarajaiah, S., Reinhorn, A. M., and Constantinou, M. C. (1989). "Nonlinear Dynamic Analysis of Three-Dimensional Base Isolated Structures (3D-BASIS)." Report NCEER-89-0019, National Center for Earthquake Engineering Research, University at Buffalo, United States, 132p.

Park, Y. J., Wen, Y. K., and Ang, A. H. S. (1986). "Random vibration of hysteretic systems under bi-directional ground motions." *Earthquake Engineering & Structural Dynamics*, 14(4), 543-557.

Warn, G. P. (2006). "The coupled horizontal-vertical response of elastomeric and lead-rubber seismic isolation bearings." PhD Dissertation, University at Buffalo.

Warn, G. P., Whittaker, A. S., and Constantinou, M. C. (2007). "Vertical stiffness of elastomeric and lead-rubber seismic isolation bearings." *Journal of Structural Engineering*, 133(9), 1227-1236.

Yamamoto, S., Kikuchi, M., Ueda, M., and Aiken, I. D. (2009). "A mechanical model for elastomeric seismic isolation bearings including the influence of axial load." *Earthquake Engineering & Structural Dynamics*, 38(2), 157-180.

Yang, Q. R., Liu, W. G., He, W. F., and Feng, D. M. (2010). "Tensile stiffness and deformation model of rubber isolators in tension and tension-shear states." *Journal of Engineering Mechanics*, 136(4), 429-437.